Identifying origins of and pathways for spring waters in a semiarid basin using He, Sr, and C isotopes: Cuatrociénegas Basin, Mexico

B.D. Wolaver[1,*], L.J. Crossey[2,*], K.E. Karlstrom[2,*], J.L. Banner[3,*], M.B. Cardenas[3,*], C. Gutiérrez Ojeda[4,*], and J.M. Sharp, Jr.[3,*]

[1]*Bureau of Economic Geology, University of Texas at Austin, 10100 Burnet Road, Austin, Texas 78758, USA*
[2]*Department of Earth and Planetary Sciences, University of New Mexico, MSCO3-2040, 1 University of New Mexico, Albuquerque, New Mexico 87131, USA*
[3]*Department of Geological Sciences, University of Texas at Austin, 1 University Station, Austin, Texas 78712-0254, USA*
[4]*Instituto Mexicano de Tecnología del Agua (IMTA), Paseo Cuauhnáhuac 8532, Colonia Progreso, 62550 Jiutepec, Morelos, México*

ABSTRACT

He, C, and Sr isotopes are used to infer spring sources in a water-stressed area. Spring-water origins and pathways in the Cuatrociénegas Basin are revealed by linking structure and geochemistry via regionally extensive fault networks. This study presents the first dissolved noble gas and He isotopic data from northeastern Mexico. Basement-involved faults with complex reactivation histories are important in northeastern Mexico tectonics and affect hydrogeologic systems. The importance of faults as conduits for northeastern Mexico volcanism is recognized, but connections between faulting and the hydrogeologic system have not been extensively investigated. This research tests the hypothesis that Cuatrociénegas Basin springs are divided into two general classes based upon discharge properties: (1) regional carbonate aquifer discharge (mesogenic) mixed with contributions from deeply sourced (endogenic) fluids containing ^{3}He and CO_2 from the mantle that ascend along basement-involved faults; and (2) carbonate aquifer discharge mixed with locally recharged (epigenic) mountain precipitation. Carbonate and/or evaporite dissolution is indicated by Ca-SO_4 hydrochemical facies. He isotopes range from 0.89 to 1.85 R_A (R_A is the $^{3}He/^{4}He$ of air, 1.4×10^{-6}) and have minimal ^{3}H, from which it is inferred that basement-involved faults permit degassing of mantle-derived He (to 23% of the total He) and CO_2 ($pCO_2 \leq 10^{-1}$ atm). Mantle degassing is compatible with the thinned North American lithosphere, as shown in tomographic images. Sr isotopes in both Cuatrociénegas Basin springs and spring-deposited travertine ($^{87}Sr/^{86}Sr$ = 0.707428–0.707468) indicate that carbonate rocks of the regional Cupido aquifer ($^{87}Sr/^{86}Sr$ = 0.7072–0.7076) are the main source of Sr. Rock-water interactions with mafic volcanic rocks ($^{87}Sr/^{86}Sr$ = 0.70333–0.70359) are not inferred to be an important process. Groundwater-dissolved inorganic C origins are modeled using major elements and C isotopes. C isotope data show that ~30% ± 22% of CO_2 in spring water is derived from dissolution of aquifer carbonates (C_{carb} = 30%), 24% ± 16% is from soil gas and other organic sources (C_{org} = 24%), and 46% ± 33% is from deep sources [C_{endo} (endogenic crust and mantle) = 46%]. This study demonstrates the presence of mantle-derived ^{3}He and deeply sourced CO_2 that ascend along basement-penetrating faults and mix with Cupido aquifer groundwater before discharging in Cuatrociénegas Basin springs.

INTRODUCTION

He, Sr, and C isotopes are used to identify the origins of and groundwater pathways for Cuatrociénegas Basin springs; the basin is an oasis in the Chihuahuan Desert region of northeastern Mexico (Fig. 1). Dozens of springs flank the 2300-m-high Sierra San Marcos anticline, which bisects the basin and sources critical flows to groundwater-dependent pools, streams, and marshes that are refugia for >70 endemic species (Hendrickson et al., 2008; Fig. 2). Springs have varied spatial distribution and geochemistry. Spring vents are often obscured by valley-fill alluvium, but high-discharge springs generally issue directly from fractures in Cretaceous carbonate rocks. Other springs are located at the base of alluvial fans (Wolaver and Diehl, 2011). CO_2-rich spring water with pCO_2 1.5–3 orders of magnitude higher than atmosphere facilitates deposition of rare modern freshwater stromatolites (Dinger et al., 2006).

The study area is in the Chihuahuan Desert, where long-term (1942–2003) annual precipitation of 200 mm exceeds annual potential evaporation (1964–1988) of 1960 mm (Aldama et al., 2005). Irrigated agriculture since the mid-1990s in adjacent valleys caused groundwater declines of ~1 m/yr, and the main springs that formed the initial basis for irrigated agriculture in the town of Cuatrociénegas no longer flow (Wolaver et al., 2008). In addition to supporting groundwater-dependent ecosystems with unique endemic species, the Cupido aquifer that flows to Cuatrociénegas springs supplies water to more than four million people in northeastern Mexico and is correlative to the prolific Texas Edwards-Trinity aquifer (Johannesson et al., 2004). Understanding the Cuatrociénegas Basin spring-water origins is important for both developing groundwater resources for human needs and preserving spring flow for groundwater-dependent ecosystems in similar settings.

This study tests the hypothesis that Cuatrociénegas Basin springs are divided into two classes based upon discharge and geochemical properties, which are inferred to be controlled by relationships between springs and fault conduits. The first class has characteristics that imply discharge primarily from a regional

*Emails: Wolaver: brad.wolaver@beg.utexas.edu; Crossey: lcrossey@unm.edu; Karlstrom: kek1@unm.edu; Banner: banner@mail.utexas.edu; Cardenas: cardenas@jsg.utexas.edu; Gutiérrez Ojeda: cgutierr@tlaloc.imta.mx; Sharp: jmsharp@jsg.utexas.edu

Geosphere; February 2013; v. 9; no. 1; p. 113–125; doi:10.1130/GES00849.1; 6 figures; 3 tables.
Received 30 July 2012 ♦ Revision received 23 October 2012 ♦ Accepted 24 October 2012 ♦ Published online 13 December 2012

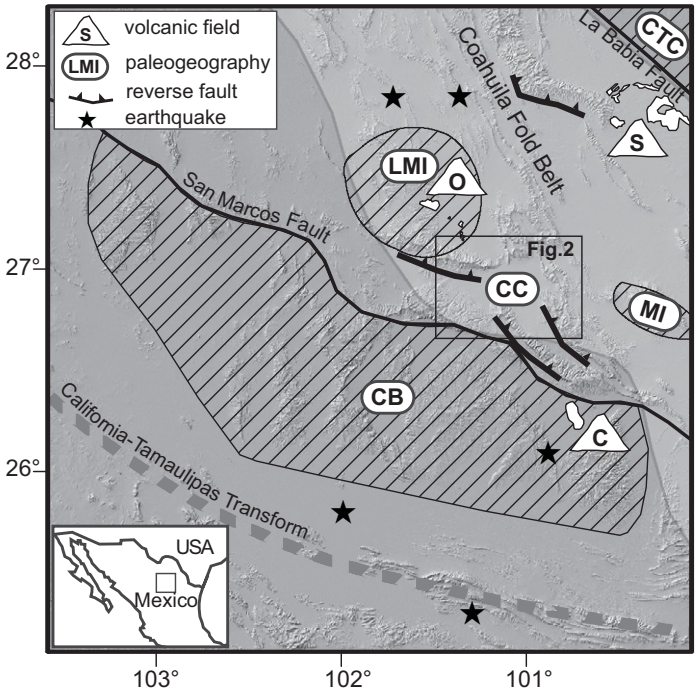

Figure 1. Study area and regional tectonic map of Cuatrociénegas Basin (CC). Relief map with topography and regional tectonic features is after Aranda-Gómez et al. (2007, 2005), Chávez-Cabello et al. (2005), Dickinson and Lawton (2001), Eguiluz de Antuñano (2001), and Goldhammer (1999). Paleogeographic elements (diagonal lines): Coahuila block (CB), La Mula Island (LMI), Monclova Island (MI), Coahuila-Texas craton (CTC). Paleotopographic highs (e.g., CB, CTC) are bounded by regional San Marcos and La Babia faults (Eguiluz de Antuñano, 2001) with intervening downthrown Sabinas Basin (light gray shaded region; Eguiluz de Antuñano, 2001). Permian–Triassic California-Tamaulipas transform is postulated structural feature (dashed line; Dickinson and Lawton, 2001). Pliocene–Pleistocene volcanic fields: Las Coloradas (C), Ocampo (O), Las Esperanzas (S) (Aranda-Gómez et al., 2007; Chávez-Cabello, 2005); volcanic fields are associated with Laramide-age reverse faults. Earthquakes are since 1973 (U.S. Geological Survey, 2009).

carbonate aquifer with some deeply sourced fluids along high-permeability fault-associated pathways. These springs have elevated discharge (≤550 L/s), elevated temperature (30–35 °C), an absence of ^{3}H, and distinctive water chemistry (high total dissolved solids, TDS > 2000 mg/L, calcite saturation, high pCO_2, mantle-derived He). The second class reflects mixing of regional carbonate aquifer and locally recharged waters. These springs have lower discharge and lower temperatures (<30 °C) and detectable ^{3}H; water chemistry shows lower TDS (500–1500 mg/L), calcite undersaturation, and less mantle-derived He.

This study also addresses spring origins and pathways using major and trace element water geochemistry and Sr and He isotope data to calculate mixing of three source waters that results in the two spring classes. The three sources are: (1) epigenic waters (dominantly younger, locally derived mountain-front precipitation); (2) mesogenic waters (older, regional carbonate aquifer groundwater); and (3) endogenic waters (inputs from deep fault systems). Isotopes of Sr in groundwater have been used to identify the source of Sr ions and to evaluate groundwater flow paths (Musgrove et al., 2010). Sr isotopes indicate that groundwater fluxes are dominated by mesogenic, regional carbonate aquifer flow. Water chemistry shows that regional carbonate aquifer water mixes with deeply derived fluids that flow along basement-penetrating faults and also mountain-front recharge, resulting in the two spring classes.

STRATIGRAPHIC AND STRUCTURAL FRAMEWORK OF NORTHEASTERN MEXICO

Cuatrociénegas Basin consists of Jurassic and Cretaceous marine and nonmarine siliciclastics overlying Precambrian to Paleozoic crystalline basement (Goldhammer, 1999; Lehmann et al., 1999). Cretaceous carbonate rocks, as thick as 800 m, form the Cupido and Aurora Formations that are the primary regional aquifer (Wolaver and Diehl, 2011; Wolaver et al., 2008). The region has a complex tectonic history with several stages of faulting (Fig. 1). During the Permian–Triassic, left-lateral motion along the Coahuila-Tamaulipas transform, associated with the opening of the Gulf of Mexico, faulted Precambrian and Paleozoic basement blocks of northeastern Mexico (Aranda-Gómez et al., 2005, 2007; Dickinson and Lawton, 2001; Goldhammer, 1999). The imprinted zones of structural weakness influenced Laramide and subsequent tectonic activity. First, extension along Neocomian normal faults (ca. 140–136 Ma) formed fault-bounded structural highs and lows, such as the Coahuila block and adjacent Sabinas Basin. Then, compression folded and faulted strata in the Paleogene (ca. 45–23 Ma; Chávez-Cabello et al., 2005). Two less intense periods of normal fault reactivation occurred in the Late Miocene to Quaternary (Aranda-Gómez et al., 2005; Chávez-Cabello et al., 2005).

The tectonic activity created faults that are critical to the area hydrogeology. Mesozoic normal faults associated with the opening of the Gulf of Mexico created conditions that permitted the deposition of Cretaceous carbonate rocks that now form a regional carbonate aquifer (Lehmann et al., 1999; Wolaver and Diehl, 2011; Wolaver et al., 2008). Paleogene reactivation of reverse faults generated the ≤3000 m anticlinal uplifts that serve as recharge areas and fractured the sedimentary rocks to create secondary permeability. Late Miocene–Quaternary normal faulting fractured the carbonate aquifer, reactivated older faulted structures, and formed foci for Pliocene–Pleistocene volcanism (Aranda-Gómez et al., 2007). Wolaver and Diehl (2011) investigated fault-associated fracture permeability influences on springs. However, previous studies did not assess the role of these faults as conduits for deeply sourced fluids.

The study area is near the boundary between the Precambrian-cored North American craton (Whitmeyer and Karlstrom, 2007) and Mesozoic accreted terranes of Mexico (Dickinson and Lawton, 2001). Northeastern Mexico is a southern continuation of a region of low mantle velocity (van der Lee and Nolet, 1997) related

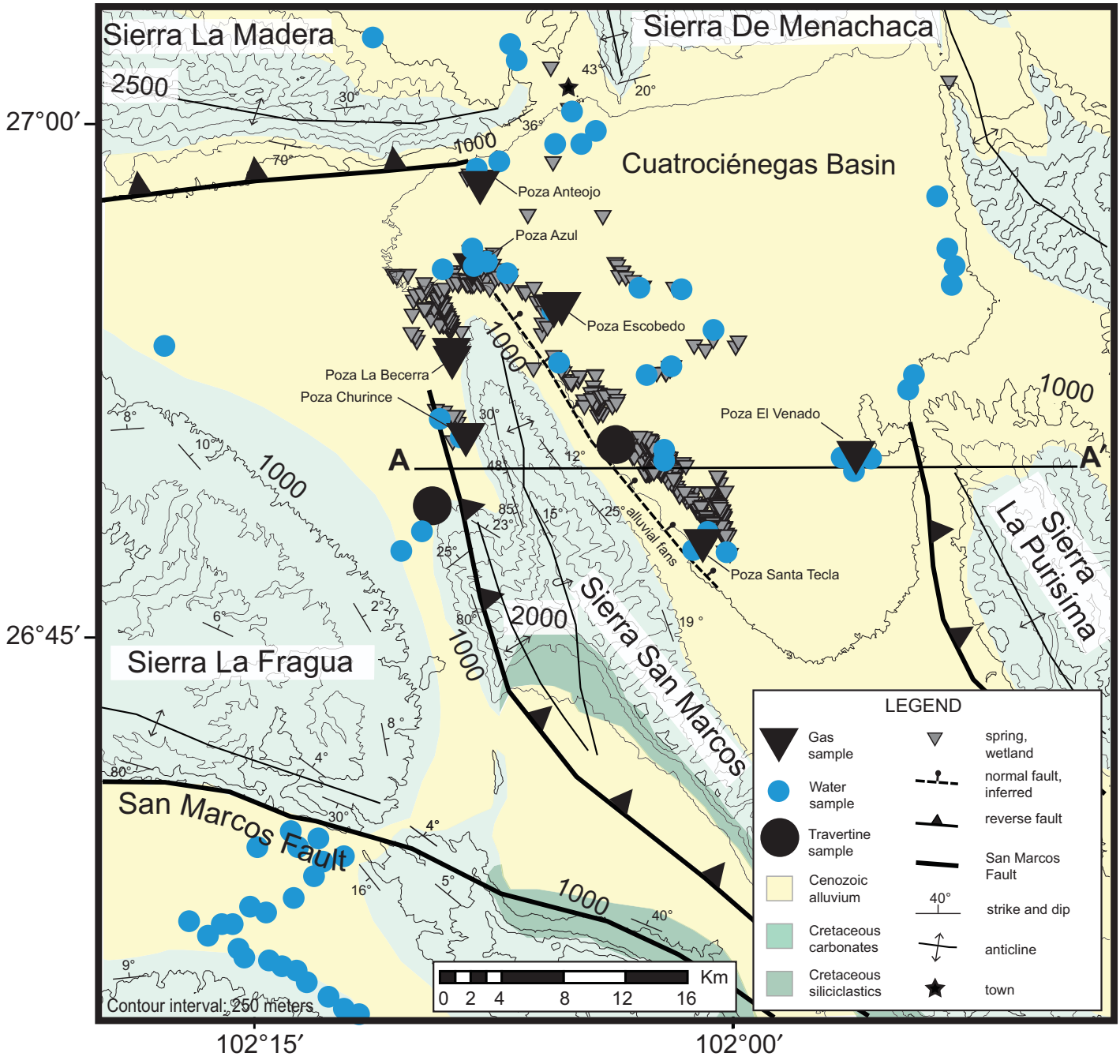

Figure 2. Cuatrociénegas Basin showing springs analyzed for dissolved gases. Spring locations (locations and map after Wolaver and Diehl, 2011) are strongly influenced by basement-involved Laramide-age reverse faults (Aranda-Gómez et al., 2007; Eguiluz de Antuñano, 2001) on the west flank of the Sierra San Marcos and an inferred normal fault on the east flank. These faults provide a mantle-derived dissolved gas conduit and account for He isotope presence. Line A–A′ shows hydrogeologic conceptual model cross section (see Fig. 6). Travertine sample locations for Sr isotopic analyses are also shown. Surface geology is from Servicio Geológico Mexicano (1998, 2008) and Chávez-Cabello et al. (2005).

to Mesozoic and ongoing mantle modification due to asthenospheric upwelling following foundering of the Farallon plate (Schmandt and Humphreys, 2010). Regions of low mantle velocity in the western United States are associated with high $^{3}He/^{4}He$ isotopic ratios in thermal spring waters (Newell et al., 2005).

Influences on regional groundwater chemistry caused by mantle degassing in areas of structural weakness have been studied using He isotopes (Crossey et al., 2006; Kennedy and van Soest, 2007; Newell et al., 2005). In Mexico, He isotopes have been used to study volcanic and hydrothermal systems (Inguaggiato et al., 2005; Taran et al., 2002; Vidal et al., 1982; Welhan et al., 1979) and for economic geology to evaluate ore fluids (Camprubí et al., 2006; Nencetti et al., 2005), but no He isotopic data are available for study area springs and groundwater to confirm the presence of deep faults in the regional carbonate aquifer.

METHODS

Analytical methods used for water chemistry, gas chemistry (e.g., He isotopes and other noble gases), C isotopes, and Sr geochemistry analyses are described in the following. Water samples were collected at springs (vents and pools), spring runs, and wells for water and gas chemistry analyses. Sr isotope geochemistry analyses were done on water samples collected from springs (vents and pools), spring runs, and travertine. Water and travertine samples were collected to provide representative samples basin-wide trends in geochemistry (Fig. 2).

Water Chemistry

Standard methods (described in Crossey et al., 2009) were used for water chemistry analyses (Table 1).

Gas Chemistry

The $^3He/^4He$ ratio is evaluated to elucidate terrigenic He crust and mantle source components by analyzing water for dissolved gases and He isotopes. Most dissolved noble gas samples were collected using passive diffusion samplers (De Gregorio et al., 2005; Gardner and Solomon, 2009). Noble gas samples were processed at the University of Utah Dissolved Gas Laboratory (following Manning and Solomon, 2003). One copper tube sample was collected from La Becerra warm vent and analyzed for $CO_2/^3He$ (methods of Poreda and Farley, 1992). The He precision is ±0.5%–1% and ±1%–2% for all other gasses. Measured $^3He/^4He$ ratios are often expressed as R/R_A, where $R = {}^3He/{}^4He$ of the sample and $R_A = {}^3He/{}^4He$ of the atmosphere (1.384×10^{-6}; Clarke et al., 1976). We report air-corrected values for total He $[He]_c$, and $^3He/^4He$ (R_C/R_A) for the non-air portion of gases dissolved in springs (using X the air-normalized He/Ne ratio correction by Hilton, 1996) by accounting for potential amounts of ^4He contributed by air and air saturated water to calculate terrigenic He (i.e., ^4He from crust and mantle sources; Solomon, 2000). The He isotopic ratios are presented compared to atmospheric concentration as R/R_A.

Carbon Isotopes

Spring water was analyzed for C isotopes using methods described by Hilton (1996). One sample (La Becerra warm vent; Table 2) was analyzed at the University of Rochester (New York), while other samples (as reported in Aldama et al., 2005) were analyzed at the University of Arizona. Methods for distinguishing CO_2 sources from water chemical data follow Chiodini et al. (2004, 2000) and Crossey et al. (2009), except an evaporite correction is used to estimate external C in high SO_4 waters (i.e., deeply derived C that flows to springs via basement-involved faults) and new methods are used to estimate dissolved inorganic C (DIC) using the computer program PHREEQC (Parkhurst, 1995).

The CO_2 sources include: (1) C_{carb} (from carbonate dissolution along flow paths); (2) C_{org} (C of organic origin); and (3) C_{endo} (endogenic CO_2 from crust and mantle). In a mass balance model, $C_{carb} = Ca^{2+} + Mg^{2+} - SO_4^{2-}$ (Chiodini et al., 2000; Fontes and Garnier, 1979). Many Cuatrociénegas Basin springs are SO_4 rich, making this calculation problematic. In cases where SO_4^{2-} is greater than $Ca^{2+} + Mg^{2+}$, C_{carb} is set to zero because there must be a sulfur source, such as H_2S. Remaining C is external carbon, where $C_{ext} = DIC_{total} - C_{carb.}$ DIC_{total} is computed from measured DIC (as alkalinity) and pH by a speciation model (PHREEQC; Parkhurst, 1995). To estimate proportions of C_{org} and C_{endo} of C_{ext}, the measured $\delta^{13}C$ is corrected for each sample by removing the isotopic proportion due to $C_{carb.}$ Depending on regions being studied, workers have used average values of 0‰ (Crossey et al., 2009; Sharp, 2007) to +2‰ (Chiodini et al., 2000; Crossey et al., 2009). The C_{ext} calculation is not especially sensitive to choice of this value, but here we use $\delta^{13}C = +0.5$‰, a central value found for the range of values (–6‰ to +5‰) of late Paleozoic southern New Mexico limestone (Koch and Frank, 2012). C_{ext} is composed of both organic components (C_{org}) and deeply sourced endogenic components (C_{endo}). Data plot within a set of binary mixing curves defined empirically by our own data, with chosen end members of (1) a soil-respired CO_2 end member with $\delta^{13}C_{org} = -28$‰ that is compatible with $\delta^{13}C_{org} = -15$‰ to –30‰ from vegetated areas (Deines et al., 1974; Robinson and Scrimgeour, 1995; Sharp, 2007) and with variable C_{ext} = 0.0001–0.004 mol/L, and (2) an endogenic CO_2 end member of $\delta^{13}C_{endo} = -3$‰ and $C_{ext} \geq 0.06$ mol/L that is comparable to values of –5‰ (Crossey et al., 2009) to –3‰ used in other studies (Chiodini et al., 2000), and comparable to a mid-oceanic ridge basalt (MORB) mantle reference value of $\delta^{13}C = -6‰ \pm 2.5‰$ (Sano and Marty, 1995).

Strontium Geochemistry

The Sr isotopes in water and travertine are evaluated to estimate relative contributions of deeply sourced Sr ions from basement faults and Sr ions derived from the regional carbonate aquifer or groundwater interactions with volcanic rocks (Table 3). An Sr-specific resin separated Sr from water and travertine samples by ion exchange (University of Texas at Austin Department of Geological Sciences Isotope Clean Laboratory; Banner and Kaufman, 1994).

RESULTS

Water Chemistry

Water chemistry data (Table 1) are compiled from published data (Johannesson et al., 2004; Aldama et al., 2005). Evans (2005) also presented water chemistry data, but focused on sampling spring discharge at spring run locations downstream of orifices.

Cuatrociénegas springs exhibit two distinct classes (Fig. 3): (1) one class plots as a grouping of Ca-SO_4–type waters (e.g., La Becerra and Escobedo springs); (2) the second class exhibits Ca-HCO_3–type waters (e.g., Santa Tecla spring).

The first class commonly discharges in springs issuing from fractures in carbonate rocks and at elevated flow rates (to 550 L/s), representing ~85% of total basin spring water (Wolaver et al., 2008). These waters have low ^3H concentrations (generally below detection limits; Table 2), TDS of 2000–3200 mg/L, and elevated temperatures (30–35 °C).

The second class has springs commonly at the base of alluvial fans with lower discharge rate, representing ~15% of total basin spring flow (Wolaver et al., 2008). These springs often have low, but measureable, ^3H (i.e., Santa Tecla has 0.2 tritium units, TU) and lower TDS (i.e., 1,415 mg/L). Spring-water temperatures are lower, but still elevated (30 °C).

Gas Chemistry

Most groundwater samples have high measured ^4He concentrations between 10^{-8} and 10^{-6} cm^3/g (Table 2). The Δ^4He, the percentage of terrigenic ^4He relative to ^4He in the atmosphere in equilibrium with water (4.31×10^{-8} cm^3/g; Giggenbach et al., 1993), ranges from 434% to 3125% with the exception of the lowest Δ^4He value (19%, sampled in an open canal; Table 2).

Springs with X factors >4 and air-corrected R_C/R_A values ranging from 1.25 R_A to 1.85 R_A (Table 2) indicate that 16%–23% of He is from MORB-type mantle sources. The highest $^3He/^4He$ values with lowest air corrections are in Poza Azul (1.84 R_A; X = 19.8), Escobedo vent (1.84 R_A; X = 21.5), and La Becerra warm vent (1.76 R_A and 1.85 R_A by two methods, X = 34 and 18.3, respectively). Gas chemistry copper tube samples (Poreda and Farley, 1992) are similar to those from passive diffusion samples from the same spring (La Becerra warm vent; Table 2).

TABLE 1. WATER CHEMISTRY AND CARBON ISOTOPES

Sample	Description	Sampled from	*T* (°C)	pH	Ca (ppm)	Mg (ppm)	Na (ppm)	K (ppm)	HCO_3 (ppm)	Cl (ppm)	SO_4 (ppm)	Charge balance (%)	SI calcite	SI dolomite	SI gypsum	Log pCO_2	$\delta^{13}C^*$ (‰)	Ref.†
Anteojo	–	spring	29.9	6.95	258.0	62.0	41.3	2.5	168.5	21.0	1034.0	–15.4	–0.11	–0.47	–0.43	–1.74		1
Azul	–	spring	33.3	7.32	316.1	108.0	180.4	7.8	228.8	95.6	1648.0	–15.1	0.43	0.77	–0.29	–1.98		1
Churnice	–	spring	31.1	7.22	283.1	97.8	154.3	7.3	201.7	102.7	1318.0	–9.8	0.24	0.40	–0.37	–1.94		1
El Venado	–	spring	28.5	6.23	65.4	13.1	18.4	0.7	263.6	16.9	68.5	–9.9	–0.97	–2.25	–1.79	–0.80		1
Escobedo (inflow canal)	–	spring	28.2	5.91	414.0	132.0	230.0	9.6	276.4	132.0	1687.0	–2.6	–0.85	–1.84	–0.19	–0.52		1
Escobedo (vent)	–	spring	35.0	6.28	372.0	116.0	191.0	8.6	190.5	107.0	1410.0	2.2	–0.56	–1.23	–0.28	–1.00		1
La Becerra (cool vent)	–	spring	32.2	7.48	378.0	119.0	174.9	8.3	214.2	87.0	1518.4	–2.1	0.63	1.15	–0.25	–2.18		1
La Becerra (warm vent)	–	spring	34.2	7.34	302.8	98.2	161.1	10.6	225.5	122.7	971.0	7.1	0.52	0.96	–0.45	–2.00	–15.4	1
Santa Tecla	–	spring	30.0	6.68	144.0	47.7	70.4	3.0	233.7	33.3	451.7	0.3	–0.37	–0.83	–0.89	–1.32		1
Precipitation	–	precipitation	20.0	6.00	14.7	1.1	5.9	3.9	38.1	3.9	13.5	7.6	–2.67	–6.18	–2.89	–1.44		2
CNA-82	El Pilar	well	28.0	8.11	629.0	197.0	504.0	12.0	126.3	249.9	2520.0	8.8	1.06	1.97	0.03	–3.13	–2.9	2
CNA-84	El Pilar	well	28.5	7.10	642.0	186.0	454.0	11.0	139.1	213.4	2544.0	6.7	0.15	0.12	0.04	–2.03		2
CNA-83	El Pilar	well	28.8	7.18	650.0	188.0	472.0	12.0	126.3	225.5	2592.0	6.9	0.19	0.21	0.05	–2.16		2
CNA-85	El Pilar	well	30.1	7.16	653.0	185.0	457.0	11.0	114.1	201.0	2568.0	7.7	0.15	0.12	0.05	–2.17		2
CNA-87	El Pilar	well	29.1	7.20	651.0	188.0	492.0	11.0	114.1	237.5	2640.0	6.5	0.17	0.16	0.05	–2.22		2
CNA-103	Beta Santa Monica 5	well	31.0	7.01	224.0	67.0	51.0	5.0	214.1	42.5	640.0	3.5	0.08	0.02	–0.64	–1.69		2
CNA-86	El Pilar	well	27.4	7.27	706.0	181.0	406.0	11.0	126.3	201.0	2540.0	8.3	0.31	0.37	0.08	–2.26		2
CNA-81	El Pilar	well	26.9	7.26	655.0	168.0	359.0	11.0	126.3	176.6	2496.0	4.0	0.26	0.28	0.06	–2.25		2
CNA104	Beta Santa Monica No. 6	well	31.8	7.01	217.0	74.0	45.0	4.0	226.9	42.5	610.0	4.8	0.10	0.14	–0.67	–1.66		2
CNA-102	Beta Santa Monica 4	well	31.2	7.65	233.0	69.0	55.0	4.0	214.1	42.5	690.0	2.4	0.71	1.29	–0.60	–2.34		2
CNA-44	Las Morenas	well	27.1	7.19	670.0	164.0	391.0	11.0	113.5	189.0	2640.0	2.3	0.15	0.03	0.08	–2.22		2
CNA-12	Buenavista	well	27.4	7.23	763.0	238.0	442.0	13.0	126.3	408.4	2900.0	3.1	0.27	0.39	0.12	–2.22		2
CNA-108	Beta Santa Monica 10	well	27.4	7.70	199.0	66.0	44.0	4.0	226.9	30.5	570.0	3.5	0.70	1.28	–0.71	–2.39	–4.0	2
CNA-90	Tanque Nuevo	well	32.1	6.99	236.0	70.0	75.0	5.0	226.9	54.6	672.0	5.4	0.11	0.09	–0.61	–1.64		2
CNA-107	Beta Santa Monica 9	well	31.3	7.21	243.0	68.0	48.0	4.0	215.3	48.6	675.0	3.2	0.31	0.45	–0.60	–1.89		2
CNA-106	Beta Santa Monica 8	well	29.5	7.93	213.0	63.0	43.0	4.0	266.0	48.6	590.0	–0.8	1.03	1.92	–0.68	–2.54		2
CNA-105	Beta Santa Monica 7	well	28.9	7.92	217.0	63.0	41.0	4.0	253.2	42.5	550.0	4.0	1.01	1.87	–0.70	–2.56		2
CNA-23	Ej. Santa Teresa de Sofia	well	29.1	7.24	358.0	104.0	151.0	6.0	215.3	140.0	1046.0	8.2	0.40	0.63	–0.37	–1.95		2
CNA-24	Ej. Santa Teresa de Sofia	well	29.6	7.28	316.0	93.0	128.0	5.0	215.3	103.5	900.0	9.5	0.42	0.68	–0.44	–1.99		2
CNA-27	Ej. Santa Teresa de Sofia	well	29.4	7.21	320.0	88.0	131.0	5.0	202.5	115.6	840.0	12.1	0.33	0.48	–0.46	–1.94		2
CNA-25	Ej. Santa Teresa de Sofia	well	28.7	7.18	383.0	105.0	212.0	6.0	215.3	164.5	1220.0	6.7	0.34	0.48	–0.30	–1.90		2
CNA-133	Santa Teresa de Sofia	well	29.7	7.28	589.0	122.0	343.0	10.0	164.7	195.0	2000.0	6.3	0.43	0.54	–0.03	–2.13		2
CNA-125	Santa Teresa de Sofia	well	33.5	7.19	215.0	63.0	69.0	4.0	240.3	73.0	575.0	3.6	0.33	0.53	–0.69	–1.81	–6.5	2
CNA-124	Santa Teresa de Sofia	well	33.4	7.16	225.0	68.0	77.0	4.0	240.3	91.5	638.0	1.5	0.30	0.49	–0.65	–1.78		2
CNA-003	Beta Santa Monica 2	well	31.1	7.28	207.0	66.0	46.0	4.0	240.3	128.0	534.0	–2.7	0.38	0.65	–0.73	–1.91		2
CNA-143	Santa Teresa de Sofia	well	32.0	7.16	253.0	92.0	261.0	8.0	228.1	213.4	930.0	5.4	0.24	0.44	–0.53	–1.82		2

(*continued*)

TABLE 1. WATER CHEMISTRY AND CARBON ISOTOPES (*continued*)

Sample	Description	Sampled from	*T* (°C)	pH	Ca (ppm)	Mg (ppm)	Na (ppm)	K (ppm)	HCO_3 (ppm)	Cl (ppm)	SO_4 (ppm)	Charge balance (%)	SI calcite	SI dolomite	SI gypsum	Log pCO_2	$\delta^{13}C$* (‰)	Ref.†
CNA-41	El Campizal	well	28.2	7.57	646.0	180.0	467.0	12.0	114.1	249.9	2621.0	4.5	0.52	0.84	0.05	–2.60		2
CNA-43	El Campizal	well	29.0	7.48	675.0	182.0	613.0	12.0	240.3	304.9	3100.0	–1.3	0.74	1.28	0.10	–2.18	–7.2	2
CNA-39	El Campizal	well	28.5	7.38	648.0	168.0	439.0	11.0	126.3	207.0	2690.0	1.8	0.38	0.53	0.07	–2.36		2
P-01	Poza Churince	spring	31.3	7.57	362.0	100.0	160.0	8.0	215.3	103.5	1230.0	2.9	0.73	1.29	–0.31	–2.28		2
CNA-144	Santa Teresa de Sofia	well	31.1	7.02	229.0	111.0	243.0	12.0	253.2	158.5	940.0	6.9	0.10	0.27	–0.57	–1.64		2
CNA-142	Santa Teresa de Sofia	well	31.5	7.01	239.0	87.0	231.0	8.0	228.1	176.6	1004.0	–0.6	0.06	0.06	–0.52	–1.67		2
CNA-100	Beta Santa Monica 1	well	30.4	7.11	258.0	72.0	57.0	4.0	228.1	54.6	750.0	1.5	0.23	0.29	–0.55	–1.77	–4.5	2
CNA-121	Canoas	well	22.9	7.37	74.0	28.0	10.0	5.0	342.2	12.1	33.0	–0.6	0.25	0.41	–2.09	–1.87		2
CNA-101	Beta Santa Monica 3	well	30.1	7.09	234.0	62.0	47.0	4.0	240.3	42.7	710.0	–3.4	0.20	0.20	–0.59	–1.73		2
CNA-233	A.P. Nueva Atalaya	well	32.5	7.06	376.0	101.0	159.0	7.0	266.0	91.5	1280.0	1.2	0.34	0.51	–0.29	–1.66	–5.5	2
CNA-241	Papalote Nueva Atalaya	well	29.7	7.76	363.0	117.0	154.0	9.0	253.2	79.1	1240.0	5.1	0.96	1.81	–0.32	–2.41		2
P-02	Poza La Becerra	spring	32.1	7.24	377.0	115.0	160.0	8.0	240.3	91.5	1296.0	3.9	0.47	0.82	–0.29	–1.89		2
P-03	Poza Escobedo	spring	34.5	7.42	393.0	108.0	160.0	8.0	253.2	91.5	1340.0	2.0	0.71	1.27	–0.27	–2.03		2
P-04	Poza Azul I	spring	27.8	7.90	400.0	131.0	193.0	9.0	228.1	109.8	1455.0	4.0	1.04	1.95	–0.24	–2.62		2
CNA-216	Antiguos Mineros del Norte	well	32.6	6.96	217.0	57.0	74.0	4.0	278.8	48.8	560.0	4.2	0.16	0.14	–0.70	–1.51		2
CNA-178	El Nogalito	well	24.3	6.79	254.0	81.0	41.0	3.0	303.8	97.5	576.0	4.5	–0.02	–0.21	–0.64	–1.37		2
P-05	Poza Santa Tecla	spring	31.7	7.24	153.0	44.0	47.0	3.0	253.2	30.5	350.0	5.1	0.30	0.45	–0.95	–1.83		2
P-06	Poza Orozco	spring	31.2	7.63	378.0	103.0	159.0	8.0	215.3	91.5	1240.0	5.2	0.80	1.43	–0.30	–2.34		2
P-07	Poza Azul	spring	31.2	7.15	394.0	113.0	167.0	8.0	266.0	91.5	1276.0	5.7	0.44	0.71	–0.28	–1.76		2
P-08	Poza Las Tortugas	spring	26.8	7.75	370.0	125.0	265.0	13.0	253.2	140.0	1400.0	5.7	0.90	1.68	–0.28	–2.42		2
CNA-186	Rancho Los Alamos	well	28.7	6.48	229.0	65.0	34.0	2.0	316.6	67.0	543.0	–0.3	–0.29	–0.75	–0.69	–1.00	–8.3	2
CNA-199	EL Jonuco	well	26.6	6.75	367.0	103.0	46.0	2.0	240.3	36.5	1008.0	7.3	–0.05	–0.30	–0.35	–1.42		2
CNA-250	Papalote San Lorenzo	well	30.3	7.20	377.0	124.0	156.0	11.0	278.8	79.1	1234.0	7.2	0.48	0.86	–0.31	–1.80		2
CNA-227	Las Carpas	well	27.0	7.07	102.0	13.0	7.0	1.0	278.8	9.9	40.0	7.0	0.06	–0.39	–1.87	–1.63		2
CNA-252	La Vega	spring	25.7	7.22	92.0	11.0	2.0	1.0	202.5	8.0	82.5	3.5	0.01	–0.55	–1.58	–1.93	–11.0	2
CNA-243	El Venado	spring	29.7	7.23	88.0	15.0	15.0	1.0	189.7	24.4	87.5	6.2	0.02	–0.33	–1.59	–1.94		2
P-09	Rio Mezquites	spring run	31.3	7.82	330.0	128.0	213.0	11.0	266.0	115.6	1225.0	6.6	1.02	2.01	–0.37	–2.44		2
CNA-191	ETA 8	well	24.2	6.73	271.0	108.0	57.0	2.0	342.2	61.0	768.0	4.4	–0.04	–0.16	–0.54	–1.26		2
P-10	San Josedel Anteojo	spring	30.4	7.22	323.0	62.0	9.0	2.0	215.3	12.3	800.0	3.7	0.41	0.48	–0.44	–1.91		2
P-11	Las Playitas	spring run	26.8	8.32	550.0	216.0	430.0	20.0	114.1	219.5	2560.0	3.5	1.13	2.20	–0.01	–3.41		2
P-12	Poza Ramon Manriquez	spring run	30.3	8.17	612.0	280.0	409.0	21.0	289.5	244.8	2562.0	7.4	1.48	3.00	–0.01	–2.83		2
P-13	Posa Los Hundidos	spring run	30.1	7.35	798.0	353.0	529.0	27.0	319.6	318.0	3264.0	8.8	0.82	1.65	0.13	–1.94		2
P-14	Poza Azul 11	spring	32.1	7.48	240.0	71.0	103.0	6.0	206.2	70.0	855.0	–2.0	0.52	0.91	–0.54	–2.18		2
P-15	Los Riachuelos	spring run	32.8	8.09	679.0	539.0	844.0	53.0	180.6	545.0	4520.0	2.5	1.16	2.61	0.11	–2.96		2
P-16	Tierra Blanca	spring	31.6	7.18	350.0	108.0	158.0	10.0	231.2	101.0	1266.7	1.0	0.36	0.60	–0.32	–1.84		2
P-17	El Mojarral	spring run	33.2	7.30	340.0	100.0	145.0	9.0	209.2	94.7	1196.7	1.6	0.46	0.78	–0.34	–2.00		2
P-18	Poza XYZ	spring	29.5	7.99	484.0	138.0	195.0	13.0	173.2	130.0	1800.0	0.5	1.07	1.96	–0.12	–2.84		2
CNA-161	Ampuero 6	well	23.7	6.83	414.0	288.0	293.0	6.0	316.0	532.0	1613.3	4.1	0.06	0.28	–0.27	–1.43		2
P-19	Poza Los Gueros	spring	24.9	8.07	377.0	12.0	173.0	7.0	184.2	103.0	1256.7	–10.0	1.08	0.99	–0.24	–2.89		2
P-20	Laguna Churince	spring run	28.9	7.70	426.0	122.0	182.0	8.0	167.8	113.0	1460.0	5.7	0.76	1.34	–0.21	–2.54		2
CNA-112	Beta Santa Monica 14	well	32.6	6.86	188.0	61.0	51.0	4.0	288.7	39.2	528.0	–0.4	0.02	–0.04	–0.76	–1.40		2

(*continued*)

TABLE 1. WATER CHEMISTRY AND CARBON ISOTOPES (*continued*)

Sample	Description	Sampled from	*T* (°C)	pH	Ca (ppm)	Mg (ppm)	Na (ppm)	K (ppm)	HCO_3 (ppm)	Cl (ppm)	SO_4 (ppm)	Charge balance (%)	SI calcite	SI dolomite	SI gypsum	Log pCO_2	$\delta^{13}C$* (‰)	Ref.†
CNA-119-B	Rancho La Ximena	spring	27.4	7.23	74.0	24.0	23.0	2.0	273.3	15.5	59.5	4.7	0.07	0.03	–1.84	–1.80		2
CNA-162	Ampuero 5	well	24.7	7.02	189.0	66.0	68.0	1.0	278.8	123.6	332.0	10.2	0.10	0.09	–0.93	–1.62		2
CNA-115 (25 m)	El Pilar	well	30.2	8.85	411.0	154.0	35.0	10.0	37.2	188.1	1929.0	–20.5	1.02	1.99	–0.15	–4.52		2
CNA-115 (39 m)	El Pilar	well	28.7	8.23	495.0	182.0	38.0	11.0	68.9	186.6	2088.0	–13.7	0.86	1.65	–0.07	–3.51		2
CNA-115 (64 m)	El Pilar	well	28.8	7.48	535.0	198.0	37.0	10.0	97.6	187.0	2280.0	–14.7	0.33	0.59	–0.03	–2.56		2
CNA-115 (95 m)	El Pilar	well	28.9	7.54	525.0	181.0	360.0	13.0	97.6	187.0	2270.0	3.8	0.37	0.65	–0.05	–2.62		2
CNA-129 (24 m)	Florentino Rivero	well	26.5	8.21	536.0	1278.0	9.7	287.0	106.5	9240.0	12600.0	–75.5	0.64	2.00	0.16	–3.37		2
CNA-129 (30 m)	Florentino Rivero	well	28.8	8.51	600.0	1536.0	10.3	380.0	101.7	9360.0	14400.0	–73.7	0.91	2.58	0.22	–3.74		2
CNA-129 (40 m)	Florentino Rivero	well	27.2	7.90	642.0	1908.0	10.8	500.0	138.3	9360.0	16590.0	–70.6	0.50	1.82	0.26	–2.94		2
CNA-129 (60 m)	Florentino Rivero	well	27.7	8.01	1058.0	3105.0	15.8	870.0	213.9	14100.0	26175.0	–70.6	0.93	2.68	0.53	–2.89		2
CNA-129 (70 m)	Florentino Rivero	well	27.7	7.97	707.0	2010.0	11.2	542.0	218.0	9750.0	17550.0	–70.5	0.80	2.40	0.31	–2.81		2
CNA-129 (85 m)	Florentino Rivero	well	26.6	8.31	707.0	2123.0	11.4	533.0	225.3	9975.0	17850.0	–69.7	1.10	3.01	0.31	–3.19		2
CNA-129 (100 m)	Florentino Rivero	well	26.1	8.41	780.0	2055.0	11.4	571.0	207.4	9900.0	17400.0	–68.8	1.18	3.13	0.35	–3.35		2
P-21	La Teclita	spring	31.3	7.23	133.0	40.0	41.0	3.0	241.6	29.6	311.4	2.6	0.22	0.31	–1.03	–1.84		2
CNA-227	Las Carpas	well	27.6	7.23	107.0	18.0	10.0	1.2	254.6	6.9	103.0	6.2	0.18	–0.03	–1.47	–1.83		2
CNA-225	Las Carpas	well	24.9	7.46	105.0	17.0	6.0	1.2	259.5	5.4	91.3	5.1	0.38	0.32	–1.52	–2.07		2
CNA-228	Las Carpas	well	26.4	7.26	108.0	18.0	8.0	1.1	260.3	7.0	103.0	5.1	0.21	0.01	–1.47	–1.86		2
CNA-229	San Vicente	well	26.2	7.23	126.0	18.0	16.0	1.5	250.5	11.9	172.0	3.3	0.20	–0.09	–1.22	–1.85		2
CNA-252	Las Vegas	spring	26.1	7.21	105.0	16.0	3.0	0.9	264.3	3.0	80.0	5.3	0.16	–0.13	–1.57	–1.80		2
Manantial	Cueva del Venado	spring	29.3	7.17	96.9	18.0	18.0	1.2	245.6	22.0	83.1	6.0	0.10	–0.14	–1.60	–1.77		2
CNA-243	El Venado	spring	30.0	6.87	98.6	18.0	22.0	1.3	260.3	26.2	83.2	5.0	–0.16	–0.66	–1.59	–1.44		2
CNA-37	El Hundido	well	26.9	7.33	602.0	670.0	3.7	298.0	2080.4	2880.0	6720.0	–62.7	1.26	2.91	0.12	–1.13		2
CNA-37	El Hundido	well	26.5	7.37	688.0	1098.0	5.4	394.0	1144.5	4069.3	10454.3	–63.1	1.01	2.57	0.24	–1.45		2
CNA-37	El Hundido	well	28.0	7.55	540.0	2177.0	6.8	510.0	293.4	4671.4	16457.1	–59.5	0.43	1.81	0.19	–2.24		2
CNA-37	El Hundido	well	27.2	7.24	590.0	10800.0	14.8	940.0	613.5	7280.0	61100.0	–50.9	0.25	2.10	0.38	–1.70		2
CNA-37	El Hundido	well	27.4	7.06	594.0	18000.0	22.6	132.0	846.2	9300.0	100200.0	–56.8	0.17	2.16	0.48	–1.40		2
CNA-139 (21 m)	Florentino Rivero	well	28.0	7.82	528.8	115.0	1.1	52.0	107.9	649.6	2728.0	–48.1	0.64	0.96	0.02	–2.87		2
CNA-139 (26 m)	Florentino Rivero	well	27.4	7.82	528.0	468.0	4.7	173.0	136.4	3060.0	7560.0	–73.2	0.49	1.28	0.13	–2.80		2
CNA-139 (36 m)	Florentino Rivero	well	27.9	7.71	540.0	945.0	8.1	325.0	195.5	5550.0	13575.0	–78.1	0.43	1.45	0.20	–2.55		2
CNA-139 (50 m)	Florentino Rivero	well	27.2	7.63	552.0	2178.0	9.8	429.0	207.3	6360.0	20040.0	–70.3	0.31	1.56	0.24	–2.47		2
CNA-139 (66 m)	Florentino Rivero	well	26.3	7.61	587.0	2160.0	9.6	425.0	222.8	6300.0	19980.0	–69.9	0.34	1.58	0.26	–2.43		2
CNA-139 (69 m)	Florentino Rivero	well	26.6	7.64	794.0	2650.0	11.7	498.0	231.9	6500.0	20437.5	–61.8	0.52	1.90	0.38	–2.46		2
Poza El Anteojo (10 m)	San Josedel Anteojo	well	27.3	7.05	285.0	58.0	157.0	3.0	218.2	10.8	698.0	21.4	0.16	–0.01	–0.53	–1.75		2
Poza El Anteojo (17 m)	San Jose del Anteojo	well	26.5	7.07	277.0	58.0	166.0	3.0	211.9	10.7	692.0	22.0	0.15	–0.04	–0.54	–1.79		2
CNA-170B-1 (50 m)	Rancho La Ximena	well	24.3	7.36	81.0	21.0	81.0	1.0	305.5	10.5	31.3	22.8	0.24	0.25	–2.08	–1.90		2
CNA-170B-2 (80 m)	Rancho La Ximena	well	24.3	7.52	80.0	21.0	84.0	1.0	314.0	9.9	30.2	22.5	0.41	0.58	–2.11	–2.05		2
Laguna del Garabatal	Laguna del Garabatal	spring run	18.6	7.50	393.0	124.0	186.0	11.0	180.0	121.0	1547.0	–0.7	0.42	0.59	–0.20	–2.36		3
Poza de La Becerra	Poza de La Becerra	spring	32.4	6.92	360.0	105.0	142.0	14.8	200.0	104.0	1262.0	1.4	0.07	–0.01	–0.31	–1.64		3
Pozos Bonitos	Pozos Bonitos	spring	26.2	7.03	440.0	54.0	140.0	9.3	171.0	108.0	1250.0	1.8	0.12	–0.33	–0.21	–1.86		3
Laguna Anteojo	Laguna Anteojo	spring run	26.2	6.94	232.0	63.0	29.0	5.3	190.0	17.0	706.0	–0.5	–0.10	–0.42	–0.58	–1.70		3

Note: SI—saturation index; *T*—temperature; dash in Description column indicates no additional description is needed.
*Water $\delta^{13}C$, with exception of La Becerra from Aldama et al. (2005). Where $\delta^{13}C$ is blank, not reported.
†References: 1—this study; 2—Aldama et al. (2005); 3—Johannesson et al. (2004).

TABLE 2. GAS CHEMISTRY

Sample	Elev. (m)	pH	TDS (mg/L)	T (°C)	^{3}H (TU)	Est. res. time (yr)	TDG (atm)	Excess air (cm^3/g)	^{4}He measured (cm^3/g)	Terri-genic He (cm^3/g)	Δ^{4}He (%)	^{40}Ar (cm^3/g)	^{84}Kr (cm^3/g)	^{129}Xe (cm^3/g)	^{20}Ne (cm^3/g)	R/R$_A$	X	R$_C$/R$_A$
Rain**	750	n.r.	n.r.	n.r.	5.4	n.r.	n.r.	n.r.	n.r.	n.r.	n.r.	n.r.	n.r.	n.r.	n.r.	n.r.	n.r.	n.r.
Anteojo	735	6.95	1972	29.9	<0.1	>60	1.0920	0.0958	2.30×10^{-7}	1.9×10^{-7}	434	3.43×10^{-4}	4.11×10^{-8}	2.46×10^{-9}	1.97×10^{-7}	1.2	5.0	1.25
Azul	730	7.32	3032	33.0	<0.1	>60	1.4010	0.0346	1.12×10^{-6}	1.1×10^{-6}	2499	3.90×10^{-4}	4.65×10^{-8}	2.79×10^{-9}	2.41×10^{-7}	1.8	19.8	1.84
Churince	745	7.22	2382	31.1	<0.1	>60	1.0580	0.0506	3.01×10^{-7}	2.6×10^{-7}	598	3.01×10^{-4}	3.45×10^{-8}	2.13×10^{-9}	1.78×10^{-7}	1.3	7.2	1.35
El Venado	722	6.23	551	28.5	1.1	>60	0.9590	0.1035	3.38×10^{-7}	2.9×10^{-7}	684	2.92×10^{-4}	3.51×10^{-8}	2.01×10^{-9}	1.63×10^{-7}	0.9	8.8	0.89
Escobedo inflow canal	703	5.91	3564	28.2	<0.1	>60	0.9720	0.1554	5.11×10^{-8}	8.0×10^{-9}	19	2.86×10^{-4}	3.38×10^{-8}	2.07×10^{-9}	1.64×10^{-7}	1.1	1.3	1.41
Escobedo vent	703	6.28	3197	35.0	0.4	>60	1.6450	0.1020	1.39×10^{-6}	1.3×10^{-6}	3125	4.64×10^{-4}	5.57×10^{-8}	3.20×10^{-9}	2.76×10^{-7}	1.8	21.5	1.84
La Becerra cooler vent	765	7.48	2853	32.2	0.3	>60	1.3150	0.0367	7.61×10^{-7}	7.2×10^{-7}	1666	3.92×10^{-4}	4.54×10^{-8}	2.83×10^{-9}	2.37×10^{-7}	1.6	13.7	1.65
La Becerra hot vent	768	7.34	2999	34.2	<0.1	>60	1.2580	0.0311	9.46×10^{-7}	9.0×10^{-7}	2095	3.61×10^{-4}	4.16×10^{-8}	2.61×10^{-9}	2.20×10^{-7}	1.8	18.3	1.85
La Becerra hot vent copper tube†	768	7.34	2999	34.2	n.r.	n.r.	n.r.	n.r.	8.02×10^{-7}	7.79×10^{-7}	n.r.	n.r.	n.r.	n.r.	n.r.	1.8	34.3	1.76
Santa Tecla	714	6.68	1415	30.0	0.2	>60	0.9560	0.0221	2.53×10^{-7}	2.1×10^{-7}	487	2.85×10^{-4}	3.32×10^{-8}	2.10×10^{-9}	1.70×10^{-7}	1.5	6.3	1.59

Note: Elev.—elevation; n.r.—not reported; TDS—total dissolved solids; TU—tritium units; Est. res. time—estimated residence time; *T*—temperature; TDG—total dissolved gas; R/R$_A$: R = ^{3}He/^{4}He of sample, R$_A$ = ^{3}He/^{4}He of atmosphere; R$_C$ = total air-corrected He.

*Rainwater sample collected in 2004 (Aldama et al., 2005).

†CO$_2$/^{3}He for La Becerra warm vent copper tube sample is 1.2×10^{10}.

All spring waters are significantly above crustal radiogenic production values of ^{3}He/^{4}He = 0.02 R$_A$ (Craig et al., 1978).

Carbon Isotopes

Water chemistry, CO$_2$/^{3}He ratios, and C isotope data elucidate different C sources contributing to CO$_2$-rich springs in the Cuatrociénegas Basin. C isotopes reported as δ^{13}C range from –15.4‰ (La Becerra warm vent) to –2.9‰ (CNA-82; Table 1).

The CO$_2$/^{3}He value for the copper tube sample (1.2×10^{10}; Table 2) is within the range of crustal CO$_2$/^{3}He (10^8 to 10^{14}; O'Nions and Oxburgh, 1988). For 117 total groundwater samples (Table 1), C$_{carb}$ from carbonate dissolution varies spring to spring, but has a mean value of 23% ± 25%. C$_{ext}$ (computed as DIC$_{total}$ – C$_{carb}$) has a mean of 77% ± 25% for 117 springs. The δ^{13}C$_{ext}$ values calculated for each groundwater sample with δ^{13}C relative to C$_{ext}$ are described by binary mixing models (Fig. 4). For 9 water samples with C isotope values, C$_{carb}$ = 30% ± 22%, C$_{org}$ = 24% ± 16%; and C$_{endo}$ = 46% ± 33%.

Strontium Geochemistry

There are 17 spring-water samples that exhibit high homogeneity, with ^{87}Sr/^{86}Sr = 0.707429–0.707468 (Table 3; Fig. 5); two samples from a travertine quarry at the southwest flank of the Sierra San Marcos (Fig. 2) with an age estimated by Aldama et al. (2005) as Pleistocene (~17,000 yr) have ^{87}Sr/^{86}Sr = 0.707448 and 0.707449. One modern travertine sample (Fig. 2) has ^{87}Sr/^{86}Sr = 0.707428. Results of Sr isotope analyses of rock samples from Cretaceous carbonate (and gypsum bearing) rocks of the regional aquifer have similar ^{87}Sr/^{86}Sr values of 0.7072–0.7076 (Fig. 5; Lehmann et al., 2000). In contrast, volcanic rocks of nearby Las Coloradas, Las Esperanzas, and Ocampo volcanic fields (Fig. 2) have much lower ^{87}Sr/^{86}Sr values, 0.70333–0.70359 (Aranda-Gómez et al., 2007; Chávez-Cabello, 2005).

DISCUSSION

Water Chemistry

The first water class is sourced from a regional carbonate aquifer (mesogenic fluids) mixed with endogenic fluids that ascend along basement-involved faults (e.g., La Becerra and Escobedo springs). The ^{3}H analyses, as indicated by levels below the detection limit, indicate regional carbonate aquifer residence times in excess of 60 yr. Ca-SO$_4$–type waters suggest rock-water inter-

TABLE 3. Sr GEOCHEMISTRY

Sample	$^{87}Sr/^{86}Sr$ values	1/Sr [1/ppb]
Water		
Anteojo	0.707432	0.0001437
Azul	0.707436	0.0000794
Churince	0.707468	0.0000723
Escobedo vent	0.707450	0.0000711
Escobedo inflow canal	0.707438	0.0000717
Escobedo outflow canal	0.707446	0.0000727
Laguna Salada	0.707429	0.0000484
Las Playitas	0.707446	0.0000440
Los Gatos marsh 1	0.707439	0.0000290
Los Gatos marsh 2	0.707435	0.0000361
Los Hundidos	0.707437	0.0000593
Mojarral Este	0.707434	0.0000718
Mojarral Oeste	0.707454	0.0000719
Río Puente Chiquito	0.707432	0.0000686
Saca Salada Canal	0.707437	0.0000735
Santa Tecla	0.707465	0.0003860
Tío Cándido	0.707451	0.0000834
Travertine		
Los Hundidos, modern age	0.707428	0.0135
Quarry, inferred Pleistocene age	0.707449	0.0689
Quarry, inferred Pleistocene age	0.707448	0.0863
Volcanic rocks		
Las Coloradas, minimum*	0.703327	n.r.
Las Coloradas, maximum*	0.703379	n.r.
Las Esperanzas, minimum†	0.70334	n.r.
Las Esperanzas, maximum†	0.70359	n.r.
Ocampo, minimum†	0.70337	n.r.
Ocampo, maximum†	0.70346	n.r.
Carbonate rocks§		
Barremian to Albian, minimum	0.7072	n.r.
Barremian to Albian, maximum	0.7076	n.r.

Note: Sr isotope results of water and travertine are normalized to an accepted NIST SRM 987 value of 0.710250. Based on the reproducibility for the standard, with a 95% confidence (= 2× the standard error of the mean), the uncertainty on a given analysis is ±0.000016. n.r. = not reported.

*Sr isotope results reported in Chávez-Cabello (2005).

†Sr isotope results reported in Aranda-Gómez et al. (2007).

§Sr isotope results reported in Bralower et al. (1997) and Lehmann et al. (2000).

actions of a limestone aquifer with concomitant gypsum dissolution in a regional flow system (Fig. 3). Gypsum dissolution in Cuatrociénegas groundwater is consistent with the presence of hundreds of meters of cyclic carbonates and evaporites (Lehmann et al., 2000; Lehmann et al., 1999).

The second water class is consistent with a regional aquifer (mesogenic fluids) source mixed with locally recharged mountain precipitation (epigenic fluids). These Ca-HCO_3–type waters have slightly higher ^3H (i.e., 0.2 TU at Poza Santa Tecla; Fig. 2) and lower TDS, reflecting shorter residence time consistent with localized flow systems. Water chemistry also reflects mixing between meteoric recharge (epigenic waters) and an SO_4-rich end member (mesogenic), consistent with dissolution and near equilibration with gypsum (Fig. 3). Canyons in the Sierra San Marcos, associated with alluvial fans (located in Cenozoic alluvium 2–4 km south of the A–A′ cross-section line in Fig. 2), permit mixing of epigenic groundwater recently derived as mountain precipitation with mesogenic groundwater from the regional carbonate aquifer that discharges along an inferred normal fault.

PHREEQC modeling of the two groundwater classes (Parkhurst, 1995) shows equilibrium pCO_2 values as high as $10^{-0.5}$ atm, indicating high CO_2 relative to meteoric waters. Alkalinity as HCO_3^- is also high (≤229 mg/L), suggesting that CO_2 degassing from endogenic fluids ascending along basement-involved faults influences basin water chemistry.

Gas Chemistry

The Δ^4He (434%–3125%; Table 2) indicates that ^4He from terrigenic sources is greater than atmosphere-sourced ^4He. Spring waters contain nonatmospheric gases from a deep endogenic fluid system (i.e., crust or mantle). However, the lowest Δ^4He value (19%) is an air-contaminated sample approaching atmospheric equilibrium from an open canal that flows into Escobedo spring.

The presence of mantle-derived fluids in spring water is supported by $^3He/^4He$ = 0.02 R_A, significantly above crustal radiogenic production values (Craig et al., 1978). Tritiogenic ^3He contribution to R/R_A values in Cuatrociénegas Basin springs is miniscule, as groundwater ^3H concentration is ≤0.4 TU and generally less than the method detection limit (≤0.1 TU; Table 2). Spring distribution relative to faults (Fig. 2; e.g., Poza Churince, Poza Azul, and Poza Anteojo springs) indicates that fluids containing appreciable mantle gases flow to a near-surface groundwater system along basement-penetrating faults.

Cuatrociénegas Basin He isotopes (R_C/R_A = 0.89–1.85; Table 2) show that western United States regional mantle degassing (Newell et al., 2005) continues into northern Mexico south of the Proterozoic Laurentia basement edge (Whitmeyer and Karlstrom, 2007). Published Mexican He isotope data (R/R_A) for volcanic, hydrothermal, and economic geology studies are consistent with mantle He degassing: 0.3–0.6 R_A (Vidal et al., 1982), 2.36–6.33 R_A (Welhan et al., 1979), 0.66–7.5 R_A (Taran et al., 2002), 1.25–2.84 R_A (Inguaggiato et al., 2005), 0.5–2.0 R_A (Camprubí et al., 2006), and 0.57–1.03 R_A (Nencetti et al., 2005). Mantle degassing along the plate margin of western Mexico is not surprising, but is also taking place in northeastern Mexico because of the importance of basement-involved faults.

Carbon Isotopes

Waters in the Cuatrociénegas Basin have high endogenic CO_2 and mantle He isotopes that show crust and mantle fluid input along basement faults into the regional aquifer. He gas transport through the mantle and crust is partly coupled to movement of CO_2/H_2O supercritical fluids (Giggenbach et al., 1993). Gas transport from the mantle is also supported by the CO_2-rich character of Cuatrociénegas springs, which have two to three orders of magnitude higher pCO_2 than air and $\delta^{13}C$ = –15.4‰ to –2.9‰.

Strontium Geochemistry

Cuatrociénegas Basin water, travertine, and carbonate rock have similar Sr isotopic ratios. Volcanic and basement rocks do not appear to be significant Sr ion sources to groundwater (Table 3; Fig. 5). Spring-water and travertine $^{87}Sr/^{86}Sr$ data show that the regional carbonate aquifer is the Sr source. Rock-water interaction of volcanic rocks and deeply sourced waters recirculated through granitic basement (Kesler and Jones, 1980–1981) do not appear to contribute measurable Sr (we use $^{87}Sr/^{86}Sr > 0.72$ for the Precambrian to Paleozoic crystalline rock Sr end member; Crossey et al., 2009). Assuming that the Pleistocene climate was cooler and

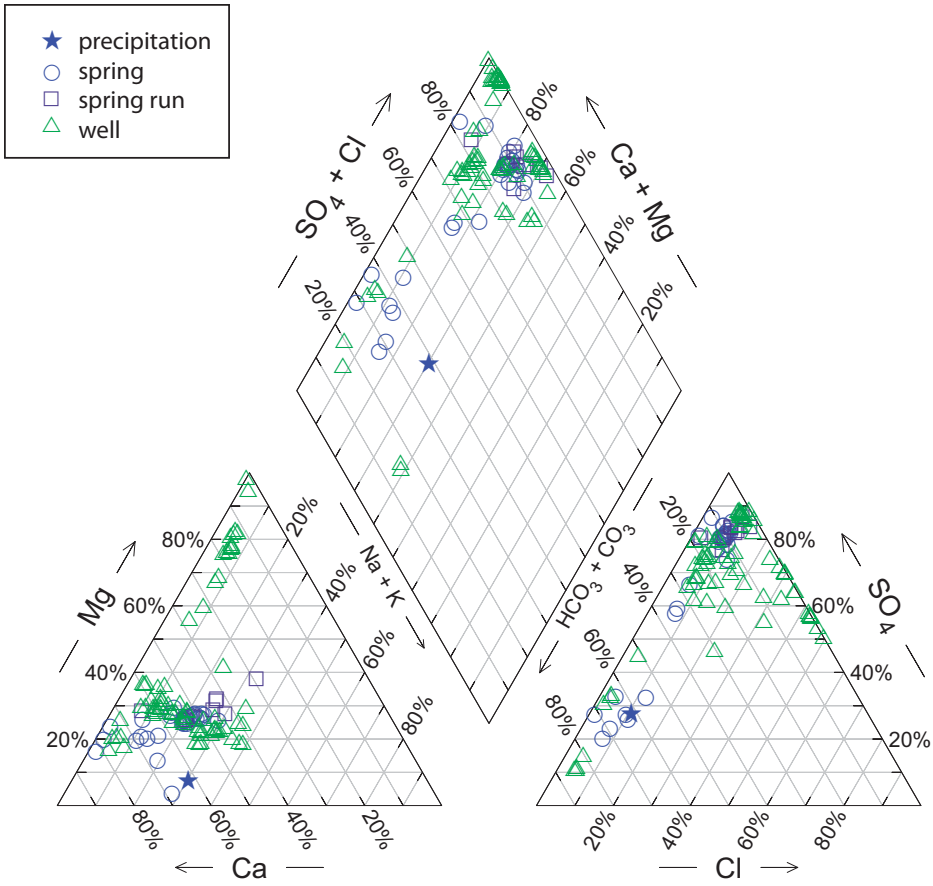

Figure 3. Piper plot of Cuatrociénegas Basin water chemistry. Cuatrociénegas Basin waters are generally of two classes: (1) primarily Ca-SO_4 water discharging from a carbonate aquifer regional flow system mixed with some fluids that ascend along basement-involved faults, and (2) Ca-HCO_3 water that is a mixture of mountain recharge and carbonate aquifer groundwater. Water chemistry data are in Table 1.

wetter, homogeneous $^{87}Sr/^{86}Sr$ from travertine of modern and inferred Pleistocene age suggest that the regional carbonate aquifer has remained the spring-water source despite drying Holocene climate (Musgrove et al., 2001). A comparison of $^{87}Sr/^{86}Sr$ in Cuatrociénegas Basin spring water with the Cretaceous section (Lehmann et al., 2000) reveals matches with the Albian Aurora and Barremian–Aptian Cupido Formations. Because the Aurora Formation is relatively thin compared to the Cupido Formation (Lehmann et al., 1999), this suggests that the Cupido Formation is the most important regional aquifer.

CONCLUSIONS AND IMPLICATIONS OF SPRING GEOCHEMISTRY ON WATER ORIGINS AND PATHWAYS

Cuatrociénegas Basin springs exhibit He, Sr, and C isotopes that indicate mixing of groundwater from the regional carbonate Cupido aquifer groundwater with endogenic sources (e.g., Poza La Becerra) and younger meteoric mountain front recharge (e.g., Poza El Venado). He, Sr, and C isotope data indicate that basement-involved faulting (1) is a critical factor controlling spring vent locations, and (2) provides conduits for circulation of deeply derived gases charged with mantle-derived ^3He and CO_2. Sr isotopes show that the Cupido aquifer is the primary Cuatrociénegas Basin spring source and the most important regional aquifer.

From the hydrogeologic conceptual model explaining groundwater, He, Sr, and CO_2 fluxes (Fig. 6), it is inferred that neotectonic extensional faults facilitate fluid ascent along reactivated, older, deeply penetrating Laramide reverse faults. The hydrogeologic conceptual model is based upon regional structural styles, hydrogeologic data, and geophysical surveys in Wolaver and Diehl (2011; refer to table 1 therein for a generalized hydrostratigraphic column).

Basin and Range–type normal faults along mountain fronts are inferred based on spring alignment on the east side of Sierra San Marcos and the presence of mantle-derived fluids in these springs. Normal faults have offsets below gravity survey resolution (Wolaver and Diehl, 2011). Normal faulting has reactivated older deeply penetrating reverse faults and provides endogenic fluid pathways. Deeper fluid conduit system components likely involve hydrothermal fluid transfer through the lithospheric mantle and lower crust.

Sr isotopes indicate that carbonate rock-water interactions dominate Cupido aquifer spring-water chemistry. Paleogene–Quaternary reactivation of basement-involved faults associated with the opening of the Gulf of Mexico generated fractures in the regional Cretaceous carbonate aquifer (Ca-SO_4 facies) that focus spring discharge ($^{87}Sr/^{86}Sr$ = 0.707429–0.707468). Basement-involved faults also provide conduits for Pliocene–Pleistocene mafic volcanism, but spring waters show no detectable contribution of Sr ions sourced from volcanic rock-water interactions (with $^{87}Sr/^{86}Sr$ = 0.70333–0.70359). A comparison of Sr isotopes from recent and inferred Pleistocene aged travertine shows that the Sr ion source to the groundwater flow system has remained the same, despite long-term climatic fluctuations. The likely dominant source of Sr ions to springs is the regionally extensive Cupido aquifer.

He isotopes show that basement-involved faults create pathways for mantle-derived gases to escape and discharge into springs ($^3He/^4He$ = 0.89–1.85 R_A). Mantle degassing is consistent with regional tomographic images that show low-velocity mantle at shallow sublithospheric depths. Similar to the western U.S. (Bethke and Johnson, 2008; Crossey et al., 2009), northern Mexico is undergoing regionally pervasive mantle degassing through CO_2-rich cool and warm springs located along faults.

Spring-water C isotopes have high dissolved CO_2 (pCO_2 = 10^{-1} to $10^{-0.3}$ compared to atmospheric concentrations of $10^{-3.5}$ atm) and alkalinity ≤230 mg/L (as HCO_3^-) and are similar to Colorado Plateau travertine-depositing springs (Crossey et al., 2006). Water chemistry analyses indicate that CO_2 is (1) 33% ± 15% C_{org}, derived from soil gas and other organic sources, (2) 30% ± 22% C_{carb}, derived from dissolution of carbonate in the aquifer, and (3) 37% ± 29% C_{endo}, derived from endogenic (i.e., deep, geologic) sources. Faults act as conduits for elevated CO_2 flux with concomitant elevated groundwater alkalinity, as observed in other North American travertine-forming springs (Bethke and Johnson, 2008; Crossey et al., 2006, 2009).

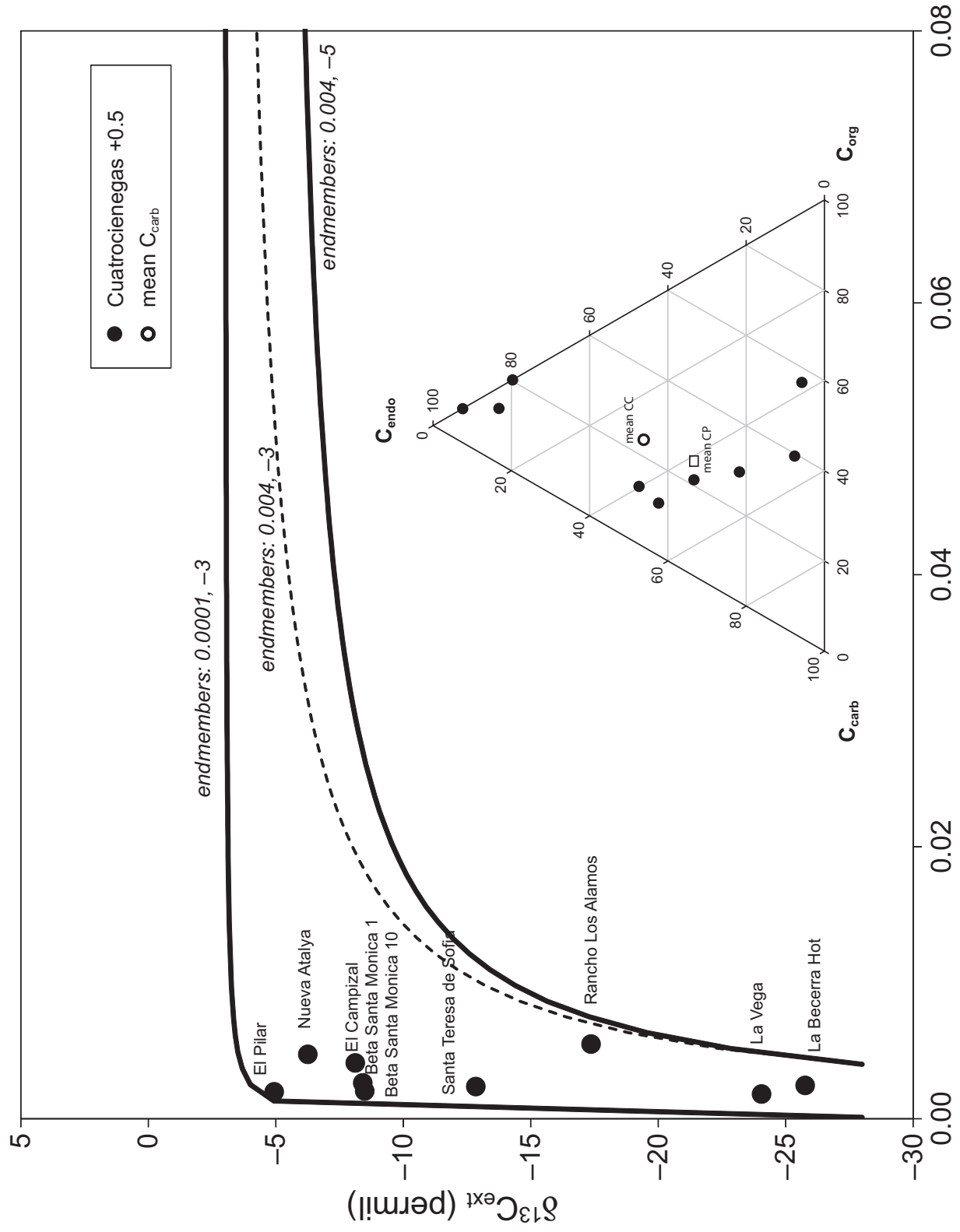

Figure 4. Chiodini plot elucidating CO_2 sources to Cuatrociénegas springs, which are CO_2 rich (pCO_2 is 2–3 orders of magnitude higher than air). CO_2 sources include: (1) C_{carb} (carbonate dissolution); (2) C_{org} (organic); and (3) C_{endo} (endogenic crust and mantle). Proportions of C_{org} and deeply sourced C_{endo} in C_{ext} (total dissolved inorganic carbon – C_{carb}) are estimated by correcting measured $\delta^{13}C$ by removing isotopic proportion due to C_{carb} (modeled as $\delta^{13}C = +0.5‰$). For nine water samples with $\delta^{13}C$, C_{carb} = 30% ± 22%, C_{org} = 24% ± 16%, and C_{endo} = 46% ± 33% (consistent with crust and mantle fluid input along basement-involved faults). CC—Cuatrociénegas; CP—Colorado Plateau.

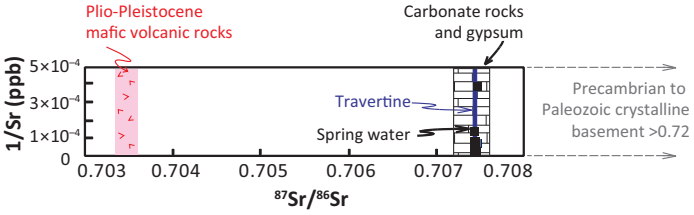

Figure 5. Ratio of $^{87}Sr/^{86}Sr$ for spring water, travertine, volcanic rocks, and carbonate rocks. Cuatrociénegas spring water $^{87}Sr/^{86}Sr$ (black squares) and Sr isotope ranges for Cuatrociénegas Basin travertine samples (blue line) and Pliocene–Pleistocene mafic volcanic rocks, carbonate rocks, and gypsum are shown. Dashed arrows (indicating $^{87}Sr/^{86}Sr > 0.72$ for Precambrian–Paleozoic crystalline rock) are after Crossey et al. (2009).

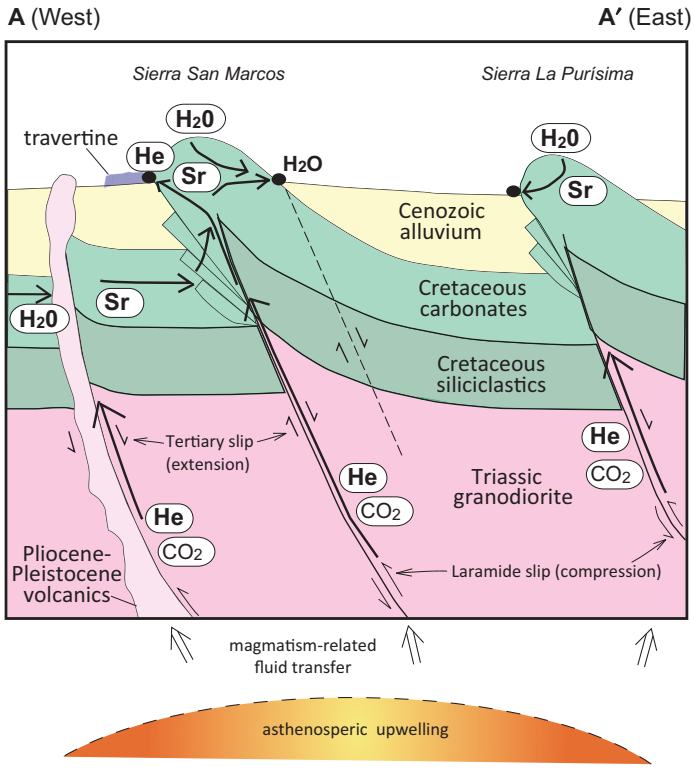

Figure 6. Hydrogeologic conceptual model showing fluxes of deeply derived He, CO_2, and Sr mixing with regional carbonate aquifer groundwater. He and CO_2 discharge along basement-involved faults, Laramide compression fault slip relative direction (lighter arrows), and extensional fault slip in Tertiary (heavier arrows), and groundwater and Sr ion fluxes in the regional carbonate aquifer and mountain recharge (heaviest arrows) are shown.

These findings on Cuatrociénegas Basin springs have implications for managing groundwater resources and endemic species. The spring waters that irrigate farms and sustain groundwater-dependent ecosystems are primarily mesogenic fluids that discharge from the Cupido aquifer with residence times in excess of 60 yr (with minor endogenic fluids). Springs also discharge a mixture of mesogenic and epigenic fluids, a combination of Cupido aquifer and mountain recharge waters. High-discharge springs in the Cuatrociénegas Basin (e.g., Azul, Churince, Escobedo, La Becerra) have geochemical characteristics of mesogenic fluids discharging from the Cupido aquifer.

ACKNOWLEDGMENTS

This study was partially funded by the the University of Texas, the Geological Society of America, BHP Billiton, the Gulf Coast Association of Geological Societies, the Houston Geological Society, and the Tinker Foundation. Larry Mack and John Lansdown provided Sr isotope and cation analyses expertise. Alan Rigby provided analytical expertise with dissolved noble gas analyses. Robert Poreda provided He isotope analyses of one of the samples. Dean Hendrickson and Suzanne Pierce collected water samples for Sr analyses. Gareth Cross, Peyton Gardner, Dean Hendrickson, Randall Marrett, Juan Manuel Rodriguez, and Vsevolod Yutsis provided helpful conversations. Laura Merner and Dawn Saepia of the Environmental Science Institute's National Science Foundation Research Experience for Undergraduates program (NSF, EAR-0552940) assisted with field work. NSF grant EAR-0838575 supported Crossey and Karlstrom's work. Publication is authorized by the Director, Bureau of Economic Geology, Jackson School of Geosciences, the University of Texas at Austin.

REFERENCES CITED

Aldama, R.A.A., and 14 others, 2005, Hydrogeologic study of the Hundido and Cuatrociénegas aquifers, Coahuila: Secretary of the Environment and Natural Resources, Mexican Institute of Water Technology, National Water Commission, National Institute of Ecology, 292 p.

Aranda-Gómez, J.J., Housh, T.B., Luhr, J.F., Henry, C.D., Becker, T., and Chávez-Cabello, G., 2005, Reactivation of the San Marcos fault during mid-to-late Tertiary extension, Chihuahua, Mexico, *in* Anderson, T.H., et al., eds., The Mojave-Sonora megashear hypothesis: Development, assessment, and alternatives: Geological Society of America Special Paper 393, p. 509–521, doi:10.1130/0-8137-2393-0.509.

Aranda-Gómez, J.J., Luhr, J.F., Housh, T.B., Valdez-Moreno, G., and Chávez-Cabello, G., 2007, Late Cenozoic intraplate-type volcanism in central and northern México: A review, *in* Alaniz-Álvarez, S.A., and Nieto-Samaniego, Á.F., eds., Geology of México: Celebrating the Centenary of the Geological Society of México: Geological Society of America Special Paper 422, p. 93–128, doi:10.1130/2007.2422(04).

Banner, J.L., and Kaufman, J., 1994, The isotopic record of ocean chemistry and diagenesis preserved in non-luminescent brachiopods from Mississippian carbonate rocks, Illinois and Missouri: Geological Society of America Bulletin, v. 106, p. 1074–1082, doi:10.1130/0016-7606(1994)106<1074:TIROOC>2.3.CO;2.

Bethke, C.M., and Johnson, T.M., 2008, Groundwater age and groundwater age dating: Annual Review of Earth and Planetary Sciences, v. 36, p. 121–152, doi:10.1146/annurev.earth.36.031207.124210.

Camprubí, A., Chomiak, B.A., Villanueva-Estrada, R.E., Canals, À., Norman, D.I., Cardellach, E., and Stute, M., 2006, Fluid sources for the La Guitarra epithermal deposit (Temascaltepec district, Mexico): Volatile and helium isotope analyses in fluid inclusions: Chemical Geology, v. 231, p. 252–284, doi:10.1016/j.chemgeo.2006.02.002.

Chávez-Cabello, G., 2005, Deformation and Cenozoic magmatism in the southern Sabinas Basin, Coahuila, México [Ph.D. thesis]: México, D.F., Universidad Nacional Autónoma de México, 266 p.

Chávez-Cabello, G., Aranda-Gómez, J.J., Molino-Garza, R.S., Cossío-Torres, T., Arvizu-Gutiérrez, I.R., and González-Naranjo, G.A., 2005, The San Marcos fault: A multireactivated northeast Mexico Jurassic basement structure, *in* Alaniz-Álvarez, S., and Nieto-Samaniego, Á.F., eds., Geology of México: Celebrating the Centenary of the Geological Society of México: GSA Special Paper 422, p. 261–286, doi: 10.1130/2007.2422(08).

Chiodini, G., Frondini, F., Cardellini, C., Parello, F., and Peruzzi, L., 2000, Rate of diffuse carbon dioxide Earth degassing estimated from carbon balance of regional

aquifers: The case of central Apennine, Italy: Journal of Geophysical Research, v. 105, no. B4, p. 8423–8434, doi:10.1029/1999JB900355.

Chiodini, G., Cardellini, C., Amato, A., Boschi, E., Caliro, S., and Frondini, F., 2004, Carbon dioxide Earth degassing and seismogenesis in central and southern Italy: Geophysical Research Letters, v. 31, L07615, doi: 10.1029/2004GL019480.

Clarke, W.B., Jenkins, W.B., and Top, Z., 1976, Determination of tritium by mass spectrometric measurements: International Journal of Applied Radiation and Isotopes, v. 27, p. 515–522, doi:10.1016/0020-708X(76)90082-X.

Craig, H., Lupton, J.E., Welhan, J.A., and Poreda, R.J., 1978, Helium isotopic ratios in Yellowstone and Lassen Park volcanic gases: Geophysical Research Letters, v. 5, p. 897–900, doi:10.1029/GL005i011p00897.

Crossey, L.J., Fischer, T.P., Patchett, P.J., Karlstrom, K.E., Hilton, D.R., Newell, D.L., Huntoon, P., Reynolds, A.C., and de Leeuw, G.A.M., 2006, Dissected hydrologic system at the Grand Canyon: Interaction between deeply derived fluids and plateau aquifer waters in modern springs and travertine: Geology, v. 34, p. 25–28, doi:10.1130/G22057.1.

Crossey, L.J., Karlstrom, K.E., Springer, A.E., Newell, D., Hilton, D.R., and Fischer, T., 2009, Degassing of mantle-derived CO2 and He from springs in the southern Colorado Plateau region—Neotectonic connections and implications for groundwater systems: Geological Society of America Bulletin, v. 121, p. 1034–1053, doi: 10.1130/B26394.1.

De Gregorio, S., Gurrieri, S., and Valenza, M., 2005, A PTFE membrane for the in situ extraction of dissolved gases in natural waters: Theory and applications: Geochemistry Geophysics Geosystems, v. 6, Q09005, doi: 10.1029/2005GC000947.

Deines, P., Langmuir, D., and Harmon, R.S., 1974, Stable carbon isotope ratios and the existence of a gas phase in the evolution of carbonate ground waters: Geochimica et Cosmochimica Acta, v. 38, p. 1147–1164, doi:10.1016/0016-7037(74)90010-6.

Dickinson, W.R., and Lawton, T.F., 2001, Carboniferous to Cretaceous assembly and fragmentation of Mexico: Geological Society of America Bulletin, v. 113, p. 1142–1160, doi:10.1130/0016-7606(2001)113<1142:CTCAAF>2.0.CO;2.

Dinger, E.C., Hendrickson, D.A., Winsborough, B.M., and Marks, J.C., 2006, Role of fish in structuring invertebrates on stromatolites in Cuatro Ciénegas, Mexico: Hydrobiologia, v. 563, p. 407–420, doi:10.1007/s10750-006-0040-4.

Eguiluz de Antuñano, S., 2001, Geologic evolution and gas resources of the Sabinas Basin in northeastern Mexico, *in* Bartolini, C., et al., eds., The western Gulf of Mexico Basin: Tectonics, sedimentary basins, and petroleum systems: American Association of Petroleum Geologists Memoir 75, p. 241–270.

Evans, S.B., 2005, Using chemical data to define flow systems in Cuatro Cienegas, Coahuila, Mexico [M.S. thesis]: Austin, University of Texas at Austin, 127 p.

Fontes, J.C., and Garnier, J.M., 1979, Determination of the initial ^{14}C activity of the total dissolved carbon: A review of the existing models and a new approach: Water Resources Research, v. 15, p. 399–413, doi:10.1029/WR015i002p00399.

Gardner, P., and Solomon, D.K., 2009, An advanced passive diffusion sampler for the determination of dissolved gas concentrations: Water Resources Research, v. 45, doi: 10.1029/2008WR007399.

Giggenbach, W.F., Sano, Y., and Wakita, H., 1993, Isotopic composition of helium, and CO_2 and CH_4 contents in gases produced along the New Zealand part of a convergent plate boundary: Geochimica et Cosmochimica Acta, v. 57, p. 3427–3455, doi:10.1016/0016-7037(93)90549-C.

Goldhammer, R.K., 1999, Mesozoic sequence stratigraphy and paleogeographic evolution of northeast Mexico, *in* Bartolini, C., et al., eds., Mesozoic sedimentary and tectonic history of north-central Mexico: Geological Society of America Special Paper 340, p. 1–58, doi: 10.1130/0-8137-2340-X.1

Hendrickson, D., Marks, J., Moline, A., Dinger, E., and Cohen, A., 2008, Combining ecological research and conservation: A case study in Cuatrociénegas, Mexico, *in* Stevens, L., and Meretsky, V., eds., Aridland springs in North America: Tucson, Arizona, University of Arizona Press, p. 127–157.

Hilton, D.R., 1996, The helium and carbon isotope systematics of a continental geothermal system: Results from monitoring studies at Long Valley caldera (California, USA): Chemical Geology, v. 127, p. 269–295, doi:10.1016/0009-2541(95)00134-4.

Inguaggiato, S., Martin-Del Pozzo, A.L., Aguayo, A., Capasso, G., and Favara, R., 2005, Isotopic, chemical and dissolved gas constraints on spring water from Popocatepetl volcano (Mexico): Evidence of gas-water interaction between magmatic component and shallow fluids: Journal of Volcanology and Geothermal Research, v. 141, p. 91–108, doi:10.1016/j.jvolgeores.2004.09.006.

Johannesson, K.H., Cortés, A., and Kilroy, K.C., 2004, Reconnaissance isotopic and hydrochemical study of Cuatro Ciénegas groundwater, Coahuila, México: Journal of South American Earth Sciences, v. 17, p. 171–180, doi:10.1016/j.jsames.2004.01.002.

Kennedy, B.M., and van Soest, M.C., 2007, Flow of mantle fluids through the ductile lower crust: Helium isotope trends: Science, v. 318, p. 1433–1436, doi:10.1126/science.1147537.

Kesler, S.E., and Jones, L.M., 1980–1981, Sulfur- and strontium-isotopic geochemistry of celestite, barite and gypsum from the Mesozoic basins of northeastern Mexico: Chemical Geology, v. 31, p. 211–224, doi:10.1016/0009-2541(80)90087-X.

Koch, J.T., and Frank, T.D., 2012, Imprint of the late Palaeozoic Ice Age on stratigraphic and carbon isotopic patterns in marine carbonates of the Orogrande Basin, New Mexico, USA: Sedimentology, v. 59, p. 291–318, doi:10.1111/j.1365-3091.2011.01258.x.

Lehmann, C., Osleger, D.A., Montañez, I.P., Sliter, W., Arnaud-Vanneau, A., and Banner, J.L., 1999, Evolution of Cupido and Coahuila carbonate platforms, Early Cretaceous, northeastern Mexico: Geological Society of America Bulletin, v. 111, p. 1010–1029, doi:10.1130/0016-7606(1999)111<1010:EOCACC>2.3.CO;2.

Lehmann, C., Osleger, D.A., and Montañez, I.P., 2000, Sequence stratigraphy of Lower Cretaceous (Barremian–Albian) carbonate platforms of northeastern Mexico: Regional and global correlations: Journal of Sedimentary Research, v. 70, p. 373–391, doi:10.1306/2DC40917-0E47-11D7-8643000102C1865D.

Manning, A.H., and Solomon, D.K., 2003, Using noble gases to investigate mountain-front recharge: Journal of Hydrology, v. 275, p. 194–207, doi:10.1016/S0022-1694(03)00043-X.

Musgrove, M., Banner, J.L., Mack, L.E., Combs, D.M., James, E.W., Cheng, H., and Edwards, R.L., 2001, Geochronology of late Pleistocene to Holocene speleothems from central Texas: Implications for regional paleoclimate: Geological Society of America Bulletin, v. 113, p. 1532–1543, doi:10.1130/0016-7606(2001)113<1532:GOLPTH>2.0.CO;2.

Musgrove, M., Stern, L.A., and Banner, J.L., 2010, Spring-water geochemistry at Honey Creek State Natural Area, central Texas: Implications for surface water and groundwater interaction in a karst aquifer: Journal of Hydrology, v. 388, p. 144–156, doi:10.1016/j.jhydrol.2010.04.036.

Nencetti, A., Tassi, F., Vaselli, O., Macías, J.L., Magro, G., Capaccioni, B., Minissale, A., and Mora, J.C., 2005, Chemical and isotopic study of thermal springs and gas discharges from Sierra de Chiapa, Mexico: Geofísica Internacional, v. 44, p. 39–48.

Newell, D.L., Crossey, L.J., Karlstrom, K.E., Fischer, T.P., and Hilton, D.R., 2005, Continental-scale links between the mantle and groundwater systems of the western United States: Evidence from travertine springs and regional He isotope data: GSA Today, v. 15, no. 12, p. 4–10, doi:10.1130/1052-5173(2005)015[4:CSLBTM]2.0.CO;2.

O'Nions, R.K., and Oxburgh, E.R., 1988, Helium, volatile fluxes and the development of continental crust: Earth and Planetary Science Letters, v. 90, p. 331–347, doi: 10.1016/0012-821X(88)90134-3.

Parkhurst, D.L., 1995, User's guide to PHREEQC—A computer program for speciation, reaction-path, advective-transport, and inverse geochemical calculations: U.S. Geological Survey Water-Resources Investigations Report 95-4227, 143 p.

Poreda, R.J., and Farley, K.A., 1992, Rare gases in Samoan xenoliths: Earth and Planetary Science Letters, v. 113, p. 129–144, doi:10.1016/0012-821X(92)90215-H.

Robinson, D., and Scrimgeour, C.M., 1995, The contribution of plant C to soil CO_2 measured using δ13C: Soil Biology and Biochemistry, v. 7, p. 1653–1656, doi:10.1016/0038-0717(95)00109-R.

Sano, Y., and Marty, B., 1995, Origin of carbon in fumarolic gas from island arcs: Chemical Geology, v. 119, p. 265–274, doi:10.1016/0009-2541(94)00097-R.

Schmandt, B., and Humphreys, E.D., 2010, Complex subduction and small-scale convection revealed by body-wave tomography of the western U.S. upper mantle: Earth and Planetary Science Letters, v. 297, p. 435–445, doi:10.1016/j.epsl.2010.06.047.

Servicio Geológico Mexicano, 1998, Carta Geológica-Minera, Tanque Nuevo G13–B69, Coahuila: Pachuca, Hidalgo, Mexico, Servicio Geológico Mexicano, scale 1:50,000.

Servicio Geológico Mexicano, 2008, Carta Geológica-Minera, Cuatro Ciénegas G13–59, Coahuila: Pachuca, Hidalgo, Mexico, Servicio Geológico Mexicano, scale 1:50,000.

Sharp, Z., 2007, Principles of stable isotope geochemistry: Upper Saddle River, New Jersey, Prentice Hall, 344 p.

Solomon, D.K., 2000, ^{4}He in Groundwater, *in* Cook, P.G., and Herczeg, A.L., eds., Environmental tracers in subsurface hydrology: Dordrecht, Kluwer Academic Publishers, p. 425–440.

Taran, Y.A., Inguaggiato, S., Marin, M., and Yurova, L.M., 2002, Geochemistry of fluids from submarine hot springs at Punta de Mita, Nayarit, Mexico: Journal of Volcanology and Geothermal Research, v. 115, p. 329–338, doi:10.1016/S0377-0273(01)00320-1.

U.S. Geological Survey, 2009, Earthquake Hazards Program: http://earthquake.usgs.gov/earthquakers/eqarchives/epic.

van der Lee, S., and Nolet, G., 1997, Upper mantle velocity structure of North America: Journal of Geophysical Research, v. 102, no. B10, p. 22815–22838, doi: 10.1029/97JB01168.

Vidal, F.V., Welhan, J., and Vidal, V.M.V., 1982, Stable isotopes of helium, nitrogen and carbon in a coastal submarine hydrothermal system: Journal of Volcanology and Geothermal Research, v. 12, p. 101–110, doi: 10.1016/0377-0273(82)90006-3.

Welhan, J.A., Poreda, R., Lupton, J.E., and Craig, H., 1979, Gas chemistry and helium isotopes at Cerro Prieto: Geothermics, v. 8, p. 241–244, doi:10.1016/0375-6505(79)90046-4.

Whitmeyer, S.J., and Karlstrom, K.E., 2007, Tectonic model for Proterozoic growth of North America: Geosphere, v. 3, p. 220–259, doi:10.1130/GES00055.1.

Wolaver, B.D., and Diehl, T.M., 2011, Control of regional structural styles and faulting on northeast Mexico spring distribution: Environmental Earth Sciences, v. 62, p. 1535–1549, doi:10.1007/s12665-010-0639-7.

Wolaver, B.D., Sharp, J.M., Jr., Rodriguez, J.M., and Flores, J.C.I., 2008, Delineation of regional arid karstic aquifers: An integrative data approach: Ground Water, v. 46, p. 396–413, doi:10.1111/j.1745-6584.2007.00405.x.